

Tissue Classification of Arterial Wall Based on Elasticity Image

Jun INAGAKI, Hideyuki HASEGAWA, Hiroshi KANAI*, Masataka ICHIKI¹ and Fumiaki TEZUKA²

Graduate School of Engineering, Tohoku University, Sendai 980-8579, Japan

¹Sendai Hospital of East Railway Company, Sendai 983-8508, Japan

²Sendai Medical Center, Sendai 980-8520, Japan

(Received November 30, 2005; accepted March 8, 2006; published online May 25, 2006)

The *phased tracking method* was developed for measuring the minute change in thickness during one cardiac cycle and the elasticity of the arterial wall. By comparing elasticity images measured by the *phased tracking method* with the corresponding pathological images, the elasticity distribution for each tissue in the arterial wall was determined. We have already measured the elasticity distributions for lipids, fibrous tissues (mixture of smooth-muscle and collagen fiber), blood clots and calcified tissues. From these previous studies, it was found that arterial tissues can be classified into soft tissues (lipids and blood clots) and hard tissues (fibrous tissue and calcified tissue) on the basis of their elasticity. However, it was difficult to differentiate lipids from blood clots and also fibrous tissue from calcified tissue. In this study, we investigated how to improve the tissue classification of the arterial wall using statistical properties of the elasticity distribution of each tissue.

[DOI: [10.1143/JJAP.45.4732](https://doi.org/10.1143/JJAP.45.4732)]

KEYWORDS: tissue classification, elasticity image, elasticity distribution, likelihood function, atherosclerosis

1. Introduction

The rupture of atherosclerotic plaques is probably the most important factor underlying the sudden outbreak of acute coronary syndrome.¹⁾ Circulatory diseases such like cerebral infarction and myocardial infarction are terminal symptoms of atherosclerosis. Therefore, the direct characterization of the composition and vulnerability of atherosclerotic plaque may offer insight into the mechanism of plaque regression and progression.^{2,3)} The elasticity of the arterial wall is largely affected by changes in the composition of the wall due to the development of atherosclerosis.⁴⁾ Therefore, the measurement of elasticity has potential for the tissue characterization of the arterial wall. For the assessment of elasticity, we have developed a method using transcutaneous ultrasound for measuring minute changes in the thickness of the arterial wall during a heart cycle^{5–13)} and the elasticity distribution of each tissue in the arterial wall.¹⁴⁾ However, the elasticity distribution of lipids is close to that of blood clots. Moreover, the elasticity distributions of fibrous tissue and calcified tissue largely overlapped each other. Such similarities are bottlenecks in the classification of tissues based on elasticity distribution.

In this study, a method of classifying tissue in the arterial wall based on statistical properties of the elasticity distribution is proposed. The proposed method improves tissue classification in comparison with that using only the mean elasticity.

2. Methods

2.1 Tissue classification based on Mahalanobis distance

For comparison with the proposed method, each pixel in an elasticity image was classified into a tissue using the squared Mahalanobis distance d_i^2 to the elasticity distribution of each tissue i ($i = 1$: lipid, 2: blood clot, 3: fibrous tissue, 4: calcified tissue). In an elasticity image, there are M ultrasonic beams and N_m pixels along m -th beam ($m = 1, \dots, M$). Therefore, in an elasticity image, there are $\sum_{m=1}^M N_m$ pixels (intervals: 75 μm in the depth direction

and 300 μm in the arterial axial direction) with respective elastic moduli, $E_{m,n}$ ($m = 1, \dots, M, n = 1, \dots, N_m$).¹²⁾ The squared Mahalanobis distance between each pixel in an elasticity image and the elasticity distribution of each tissue is obtained as follows:

$$d_i^2 = \left(\frac{E_{m,n} - \mu_i}{\sigma_i} \right)^2, \quad (i = 1, 2, 3, 4; m = 1, \dots, M; n = 1, \dots, N_m) \quad (2.1)$$

where μ_i and σ_i are the mean and standard deviation of the elasticity distribution of class i . The means and standard deviations (SD) of the elasticity distributions of respective tissues were determined to be 81 ± 40 kPa for lipids, 95 ± 56 kPa for blood clots, 1.0 ± 0.63 MPa for fibrous tissue and 2.0 ± 1.2 MPa for calcified tissue (mean \pm SD). Each pixel in the elasticity image is classified into class i which has the shortest Mahalanobis distance.

2.2 Tissue classification based on likelihood function

In this study, an elasticity image is classified using the likelihood function L_i ($i = 1$: lipid, 2: blood clot, 3: fibrous tissue, 4: calcified tissue) of the elasticity distributions. To obtain the likelihood function of the elasticity distribution of each tissue, the elasticity distribution is translated using the normal distribution to obtain the probability distribution.

From *in vitro* experiments, the elasticity distribution of each tissue, i , is obtained as illustrated in Fig. 1(a).¹⁴⁾ The elasticity distribution of each tissue consists of J_i data points with respective elastic moduli ($i = 1$: lipid, 2: blood clot, 3: fibrous tissue, 4: calcified tissue). Using all data of J_i points (J_1 : 425, J_2 : 301, J_3 : 5979, J_4 : 579) with respective elastic moduli, the ascending sequence is made for each tissue, i , as shown in Fig. 1(b). In this sequence, the j -th datum ($j = 1, \dots, J_i$) has the corresponding elastic modulus E_j ($E_j \leq E_{j+1}$) where j is named the elasticity number. It is clear in Fig. 1(a) that the mean elastic modulus of the distribution is largely different from the elastic modulus of the $(J_i/2)$ -th datum at the center of the ascending sequence. One of reasons for this is considered as follows: To obtain the elastic modulus, the change in the thickness (radial strain) of the arterial wall due to a heartbeat is measured

*E-mail address: kanai@ecei.tohoku.ac.jp

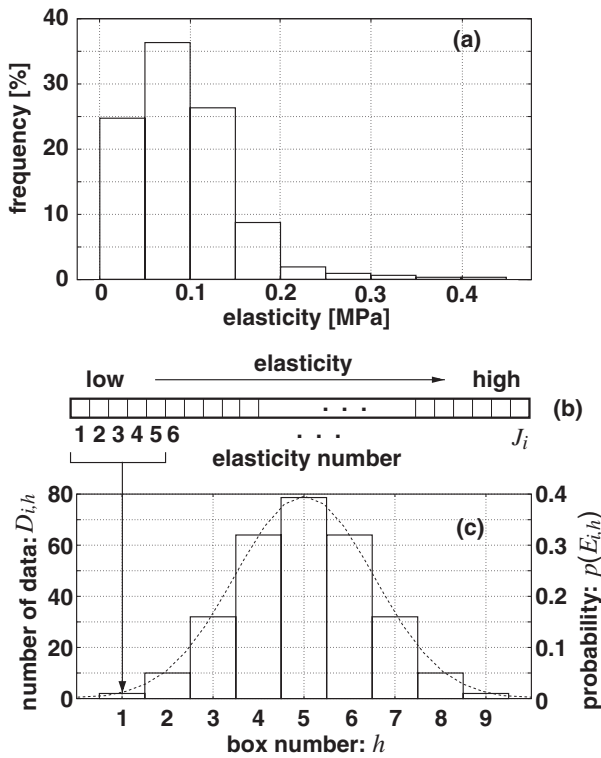


Fig. 1. Illustration of allocation of elasticities of elasticity distribution to boxes of normal distribution. (a) Original elasticity distribution of the tissue. (b) Ascending sequence of elastic modulus of elasticity distribution. (c) Normal distribution whose number of boxes correspond to that of (a).

using ultrasound. The measured change in thickness is expressed by the sum of the actual change in thickness Δh and noise e of the measurement system, and the elastic modulus is proportional to the reciprocal $1/(\Delta h + e)$ of the measured change in thickness.¹³⁾ Therefore, the variance of the estimated elastic moduli increases with decreasing actual change in thickness (increasing elastic modulus) in comparison with the case of increasing change in thickness (decreasing elastic modulus). As a result, the elasticity distribution is broadened at a high elastic modulus. Thus, as shown in Fig. 1(c), the normal distribution is assumed with respect to the elasticity number j so that the probability around the center of the ascending sequence made becomes maximum.

The probability distribution of each tissue was obtained by allocating all the data of J_i points of each tissue i to boxes of the normal distribution. The number of boxes, $\{B_i\}$, of the normal distributions is determined so that the number of data in the box for a box number, which is located at threefold the standard deviation of the box number from the mean (mean $\pm 3 \times$ SD), becomes one. As shown in Fig. 1(c), the number of data, $D_{i,h}$ ($h = 1, \dots, B_i$), included in each box is determined by following the line of the normal distribution. Then, the $(J_i/2)$ -th datum is included in the box with the highest probability.

By allocating all the data of J_i points of each tissue to boxes of the corresponding normal distribution, the mean elasticity $\bar{E}_{i,h}$ of the data included in each box is obtained. Figures 2(a-1), 2(b-1), 2(c-1), and 2(d-1) show the elasticity distributions for lipids, blood clots, fibrous tissue, and

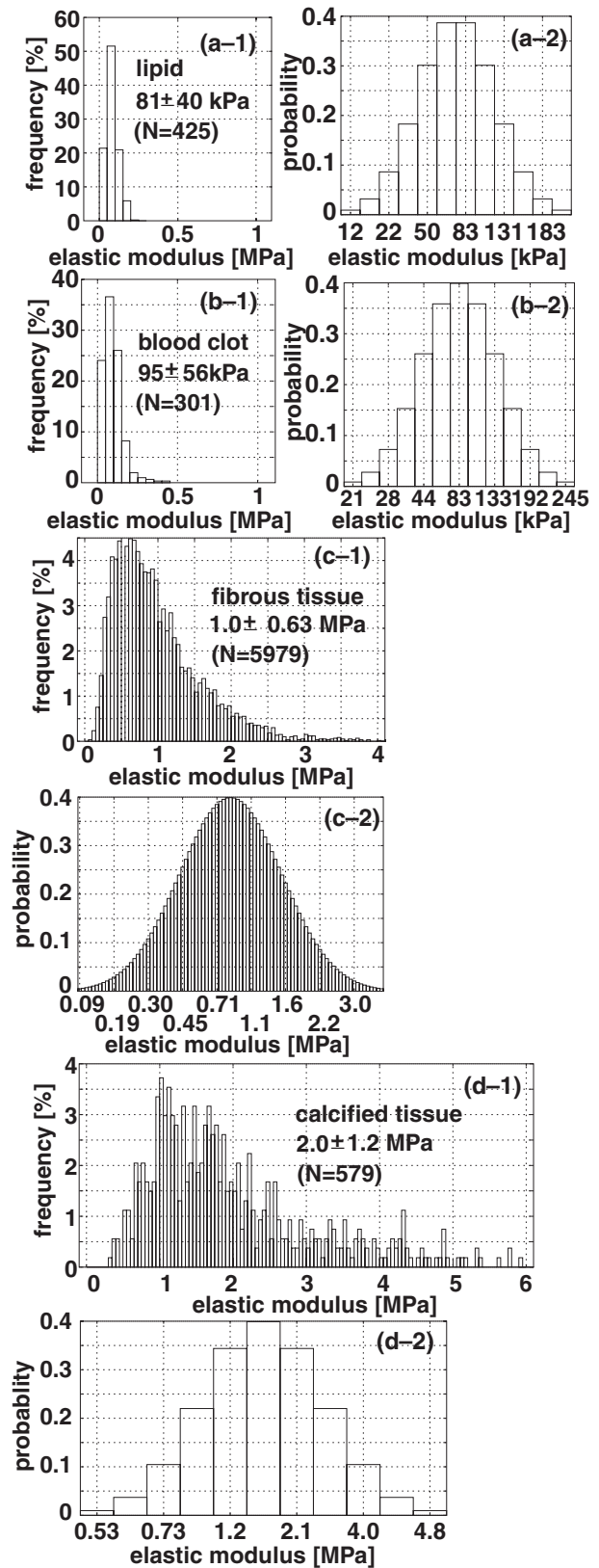


Fig. 2. Elasticity distribution and probability distribution of each tissue. (a) Lipid, (b) blood clot, (c) fibrous tissue, and (d) calcified tissue.

calcified tissue, respectively, and Figs. 2(a-2), 2(b-2), 2(c-2), and 2(d-2) show the respective probability distributions, $p_i(\bar{E}_{i,h})$, whose horizontal axis was labeled by the mean elasticity $\bar{E}_{i,h}$ of the corresponding box $B_{i,h}$.

When the elastic modulus $E_{m,n}$ measured at the depth n

along the m -th ultrasonic beam is closest to the mean elasticity $\bar{E}_{i,h}$ of the box $B_{i,h}$, the probability $p'_i(E_{m,n})$ with respect to the elastic modulus $E_{m,n}$ was determined to be $p_i(\bar{E}_{i,h})$.

For each pixel with the corresponding elastic modulus $E_{m,n}$, the region of interest (ROI) $R_{m,n}$ of $\pm 450\mu\text{m}$ in the depth direction and $\pm 450\mu\text{m}$ in the arterial axis direction is assigned. Thus, there are up to 36 elastic moduli in the ROI. Using the probability distribution $p'_i(E_{m,n})$, the log likelihood function $\ln L_i$ for the i -th class is obtained with respect to elasticities in $R_{m,n}$ as

$$\ln L_i = \sum_{(k,l) \in R_{m,n}} \ln p'_i(E_{k,l}). \quad (i = 1, 2, 3, 4) \quad (2.2)$$

However, the size of an ROI varies at the edge of an elasticity image. Therefore, we employ the log likelihood function normalized by the number of elasticities in an ROI. Thus, all pixels in an elasticity image are classified into the class that has the highest likelihood.

3. Results

3.1 Tissue classification based on Mahalanobis distance

Figures 3(a) and 3(b) show the elasticity image of the arterial wall and the corresponding pathological image, respectively. The regions of lipids, blood clots and fibrous tissue were identified by referring to the pathological image. The regions of lipids, blood clots and fibrous tissue were superimposed in Fig. 3(b) by yellow, red and blue dashed

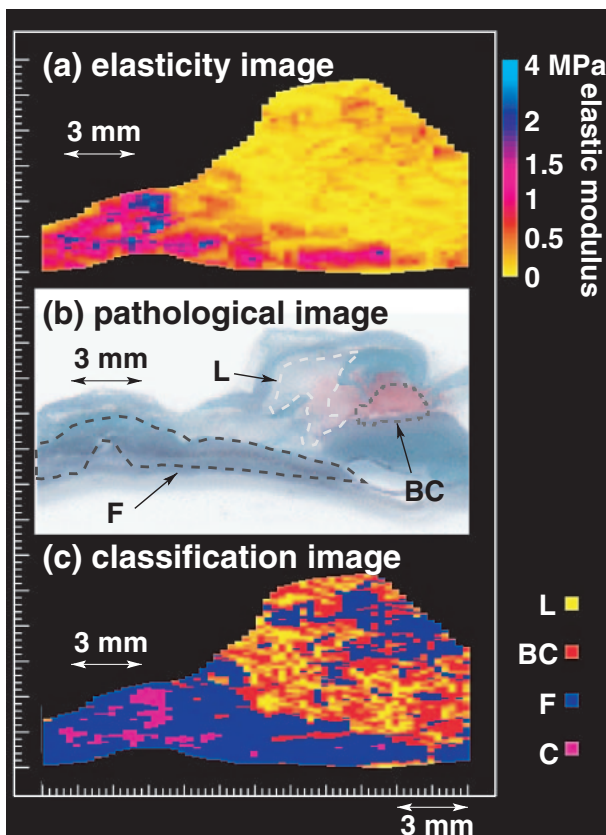


Fig. 3. (a) Elasticity image of arterial wall. (b) Pathological image of arterial wall subjected to elastica-Masson staining. (c) Tissue classification image using Mahalanobis distance (L: lipid, BC: blood clot, F: fibrous tissue, and C: calcified tissue).

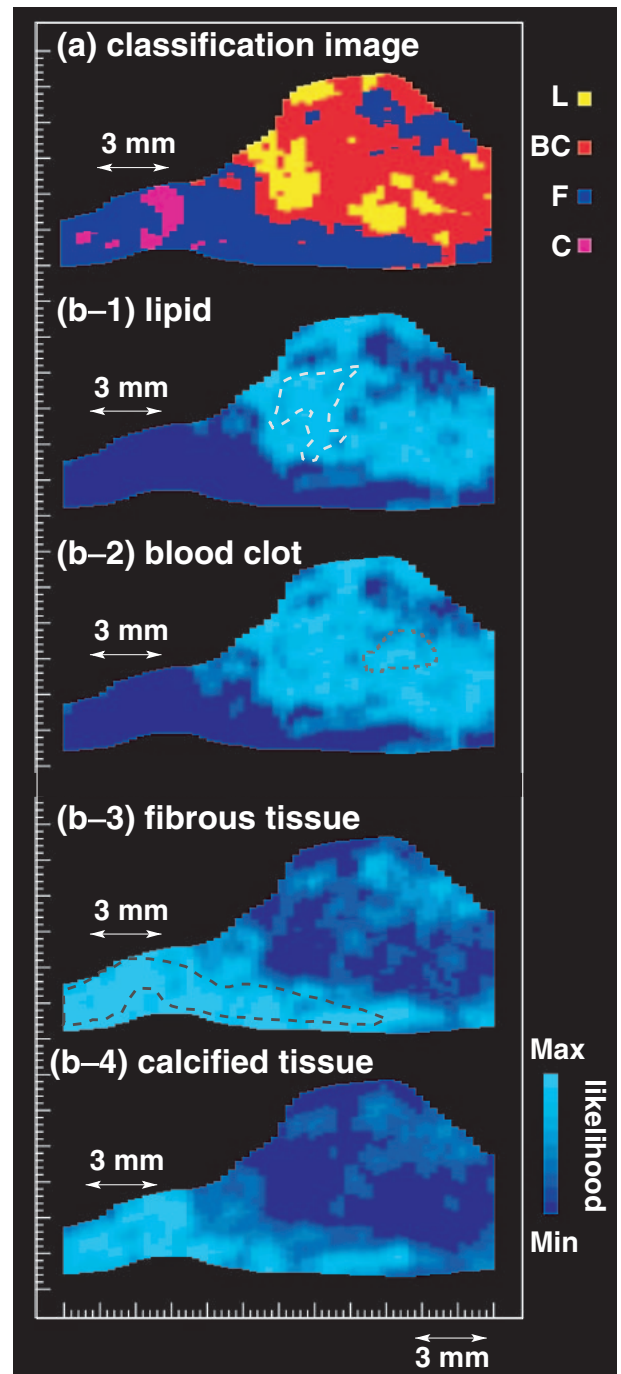


Fig. 4. (a) Tissue classification image using likelihood function of each tissue (L: lipid, BC: blood clot, F: fibrous tissue, and C: calcified tissue). (b) Likelihood image of each tissue.

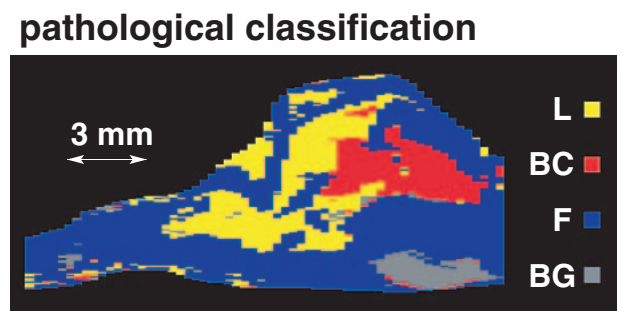


Fig. 5. Tissue classification image based on pathological image (L: lipid, BC: blood clot, F: fibrous tissue, and BG: background).

lines. Figure 3(c) shows the result of the classification based on the Mahalanobis distance between each pixel in an elasticity image and the elasticity distribution of each tissue. The regions classified as lipids, blood clots, fibrous tissue and calcified tissue were stained yellow, red, blue and purple, respectively. By comparing the pathological image and tissue classification image, misclassified pixels were distinct, particularly in regions of lipids and blood clots.

3.2 Tissue classification using likelihood function

Figure 4(a) shows the result of the classification based on the likelihood function of each tissue. Figures 4(b-1), 4(b-2), 4(b-3), and 4(b-4) show the likelihood functions L_i for lipids, blood clots, fibrous tissue and calcified tissue, respectively. The region of each tissue was indicated by dashed lines in Figs. 4(b) and 3(b). In comparison with the result of the classification based on the mean elastic modulus of each tissue shown in Fig. 3(c), misclassified regions were reduced using the likelihood function as shown in Fig. 4(a).

Figure 5 shows the tissue classification image obtained by analyzing the pathological image. The pathological image was analyzed as follows: The entire pathological image, which corresponds to the entire elasticity image, is divided into the M sections in the arterial axial direction, and each m -th section of the M sections is divided into N_m regions in the arterial radial direction. Then, each region is classified into lipids, blood clots, fibrous tissue, and calcified tissue based on RGB values in each region in the pathological image.¹⁴⁾ The regions classified as lipids, blood clots, fibrous tissue, and background were stained yellow, red, blue, and gray, respectively.

Each value in Table I is the total number of pixels classified into each tissue based on the Mahalanobis distance of each pixel with an elastic modulus and the proposed method. Each percentage shows the ratio of the number of correctly classified pixels to the corresponding total number of pixels. The correctness of the classification of each pixel was evaluated by comparing tissue classification images shown in Figs. 3(c) and 4(a) with that in Fig. 5 based on the pathological image. As shown in Table I, classification was improved using the proposed method.

Table I. Comparison of classification results with pathological findings.

	Mahalanobis distance	Proposed method
Lipid	794 (32.9%)	705 (32.9%)
Blood clot	1614 (17.4%)	2472 (21.0%)
Fibrous tissue	2590 (64.2%)	1856 (72.8%)
Calcified tissue	218 (0.0%)	183 (0.0%)

4. Conclusions

Using the likelihood function of the elasticity distribution of each tissue, the differentiation of lipids from blood clots and that of fibrous tissue from calcified tissue were improved in comparison with the classification using only the mean elasticity of each tissue.

- 1) P. R. Moreno, E. Falk, I. F. Palacios, J. B. Newell, V. Fuster and J. T. Fallon: *Circulation* **90** (1994) 775.
- 2) H. M. Loree, R. D. Kamm, R. G. Stringfellow and R. T. Lee: *Circ. Res.* **71** (1992) 850.
- 3) E. Falk, P. K. Shah and V. Fuster: *Circulation* **92** (1995) 657.
- 4) R. T. Lee, A. J. Grodzinsky, E. H. Frank, R. D. Kamm and F. J. Schoen: *Circulation* **83** (1991) 1764.
- 5) H. Kanai, M. Sato, Y. Koiwa and N. Chubachi: *IEEE Trans. Ultrason. Ferroelectr. Freq. Control* **43** (1996) 791.
- 6) H. Kanai, H. Hasegawa, N. Chubachi, Y. Koiwa and M. Tanaka: *IEEE Trans. Ultrason. Ferroelectr. Freq. Control* **44** (1997) 752.
- 7) H. Hasegawa, H. Kanai, N. Hoshimiya, N. Chubachi and Y. Koiwa: *Jpn. J. Appl. Phys.* **37** (1998) 3101.
- 8) H. Kanai, K. Sugimura, Y. Koiwa and Y. Tsukahara: *Electron. Lett.* **35** (1999) 949.
- 9) H. Kanai, Y. Koiwa and J. Zhang: *IEEE Trans. Ultrason. Ferroelectr. Freq. Control* **46** (1999) 1229.
- 10) H. Hasegawa, H. Kanai, N. Hoshimiya and Y. Koiwa: *Jpn. J. Appl. Phys.* **39** (2000) 3257.
- 11) H. Hasegawa, H. Kanai and Y. Koiwa: *Jpn. J. Appl. Phys.* **41** (2002) 3563.
- 12) H. Kanai, H. Hasegawa, M. Ichiki, F. Tezuka and Y. Koiwa: *Circulation* **107** (2003) 3018.
- 13) H. Hasegawa, H. Kanai, N. Hoshimiya and Y. Koiwa: *J. Med. Ultrason.* **31** (2004) 81.
- 14) J. Inagaki, H. Hasegawa, H. Kanai, M. Ichiki and F. Tezuka: *Jpn. J. Appl. Phys.* **44** (2005) 4593.